

Separatrix to Pedestal Density Ratio in ASDEX Upgrade H-modes Comparing DIV-I and DIV-II Operation

J. Schweinzer, K. Borrass, W. Sandmann, ASDEX Upgrade- and NBI-Teams

Max-Planck-Institut für Plasmaphysik, EURATOM Association,
Boltzmannstraße 2, D-85748 Garching

1. Introduction

Recently, there has been increased interest in the ratio of separatrix density n_s to the pedestal density n_c , because for next step devices n_s and n_c are subject to distinct constraints which might be in conflict. Therefore a reliable basis for extrapolation is necessary. A semi-empirical relation for the ratio of the separatrix density n_s to the pedestal density n_c was derived by combining experimental findings on characteristic density profile shapes with SOL physics provided by a so-called two-point model of the SOL with the assumption of Bohm-type transverse transport. [1]. This relation has been successfully applied to experimental density profiles obtained in ASDEX Upgrade (AUG) H-Mode discharges with the so called Lyra Divertor (DIV-II) [1].

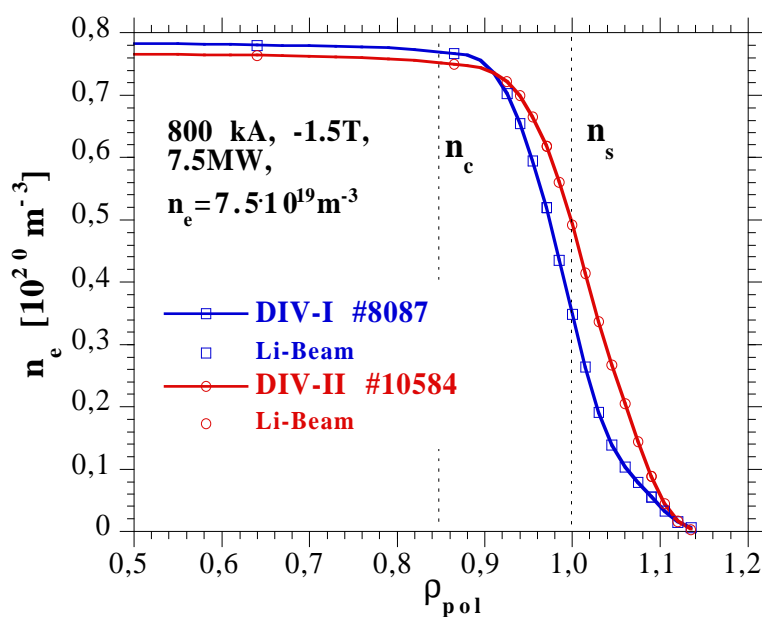


Fig. 1: Typical AUG density profiles for DIV-I and DIV-II in Type-I ELMy H-mode discharges (averaged over the ELM cycle). The line averaged densities are the same for both discharges as all global parameters too. The gradient is constant in the pedestal and near the separatrix parts of the SOL. Radial positions of separatrix and pedestal region are indicated by the broken lines. Density of symbols corresponds to spatial resolution of measurement.

SOL is increased or at least the same as for DIV-I. In fig.1 density profiles obtained by combining lithium beam edge profiles with interferometer measurements of the plasma core [4] are presented, showing the typical difference in the gradient region. One consequence of this behaviour is a difference in the ratio n_s/n_c between DIV-I and DIV-II. In this paper we study the impact of divertor geometries on the ratio n_s/n_c by extending our previous study [1] to DIV-I data.

Operation with the Lyra divertor, which is more closed than the former Divertor I (DIV-I) configuration had started in summer 1997. In general the global plasma performance and the core confinement were not significantly altered by the modification.

However, there are characteristic changes in the Scrape-Off-Layer (SOL) [2]. The closure of the divertor geometry lead to significantly increased neutral gas flux density in the private flux region. However, the relation between SOL density and neutral gas flux density in the divertor is not altered by the change from DIV-I to DIV-II [3]. Thus under all conditions the thickness of the DIV-II

2. Description of model

The discussion is guided by a model which relies largely on empirical characteristics of AUG density profiles (cf. fig. 1):

- (I) The density gradient is radially constant in the pedestal and near separatrix region, and in particular, does not jump at the separatrix.
- (II) The pedestal width δ (distance between separatrix and the innermost end of the steep gradient region) is constant.

Both features lead to a simple relation between n_s and n_c , where λ_n is the density fall-off length near the separatrix position.

$$n_c = \frac{\delta + \lambda_n}{\lambda_n} n_s \quad (1)$$

Assuming $\delta \approx \lambda_n$ (cf. fig. 1) and making use of the approximation $(1+z)/z \approx 2(1/z)^{1/2}$, with $z = \lambda_n / \delta$ one gets

$$n_c = 2 \left(\frac{\delta}{\lambda_n} \right)^{1/2} n_s \quad (2)$$

which will permit to derive relations in power law form. All other elements of the model originate from two-point models of the SOL [1 and ref. therein]. In particular estimates of the midplane temperature T_s and the temperature fall-off length λ_T are given by:

$$T_s \propto \left(\frac{q_{\perp} L^2}{\lambda_T} \right)^{2/7} \quad (3)$$

$$\lambda_T \propto \frac{n_s T_s^2}{q_{\perp} B_t} \quad (4)$$

where L is the connection length and q_{\perp} the mean power flux across the separatrix. All other quantities have already been defined or have their usual meaning. Bohm-type transverse transport was adopted in equ. 4. Finally a proportionality between λ_n and λ_T is assumed [1]. This assumption is supported by experimental findings, although no dedicated study exists so far which investigates the connection between both fall-off lengths in detail. With this assumption and with eqs. 2, 3 and 4 we get after some simple algebra

$$\frac{n_s}{n_c} \propto \frac{n_c^{7/15} (q_{95} R)^{8/15}}{q_{\perp}^{3/15} B_t^{7/15}} \quad (5)$$

Equ. 5 has the desired form and is the basis of the subsequent comparisons with experimental data. The size scaling with $R^{8/15}$ cannot be tested here, because reliable data from other machines are not available.

3. Application to DIV-I and DIV-II data

A database for Type-I ELMy H-mode discharges in DIV-I has been compiled from 24 discharges, where timeslices of stationary phases (D_2 puffed discharges with $I_p=0.6-1.2$ MA, $B_t=-2.5$ T,-1.5T, NBI: $D^0 \rightarrow D^+$, 2.5-10MW) were included, building up a set of 250 data points. The dataset for DIV-II consists of 8 discharges with combined density and power ramp-up scenarios which sum up to a total of 280 data points (D_2 puffed discharges with $I_p=0.6-$

1.0MA, $B_t = -3.0T, -1.5T$, NBI: $D^0 \rightarrow D^+$, 2.5-7.5MW) [1]. All density profiles are smoothed over ELMs and the plasma shape is the same for all discharges.

Assuming that the relevant parameters are given by equ. 5 a standard regression analysis leads to

$$n_{S,fit}^{DIV-I} = 4.35 \cdot 10^{-12} \frac{n_C^{1.51 \pm 0.09} q_{95}^{0.96 \pm 0.1}}{q_{\perp}^{-0.08 \pm 0.04} B_t^{0.35 \pm 0.07}} \quad (6)$$

where n_s and n_C in m^{-3} , q_{\perp} in W/m^2 , B_t in T and all exponents are given with their 95% confidence intervals ($R^2 = 0.85$).

The prediction of the model is given by equ. 7 where now only the coefficient of proportionality in equ. 5 is determined by a regression fit. This coefficient of proportionality C_x is different for both divertor geometries (DIV-I: $C_1 = 1.6 \times 10^{-9}$; DIV-II: $C_2 = 2.57 \times 10^{-9}$).

$$n_{S,mod}^{DIV-x} = C_x \frac{n_C^{1.47} q_{95}^{0.53}}{q_{\perp}^{0.2} B_t^{0.47}} \quad x = I, II \quad (7)$$

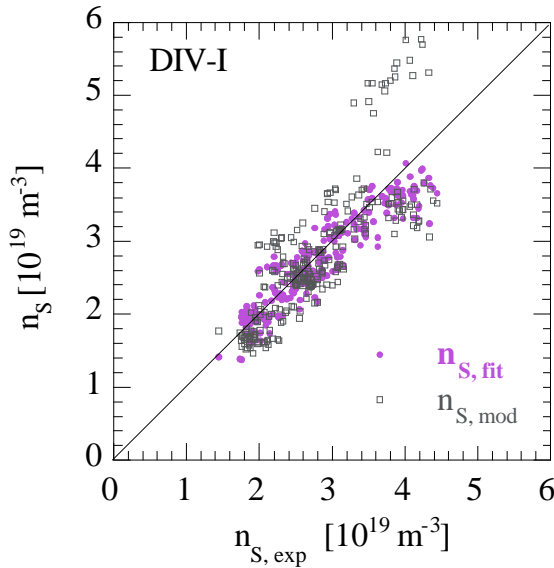


Fig. 2: Quality of both fit approaches for the DIV-I dataset. Comparison between the regression fit (equ. 6, full symbols) and the model result (equ. 7 with $x=I$, open symbols).

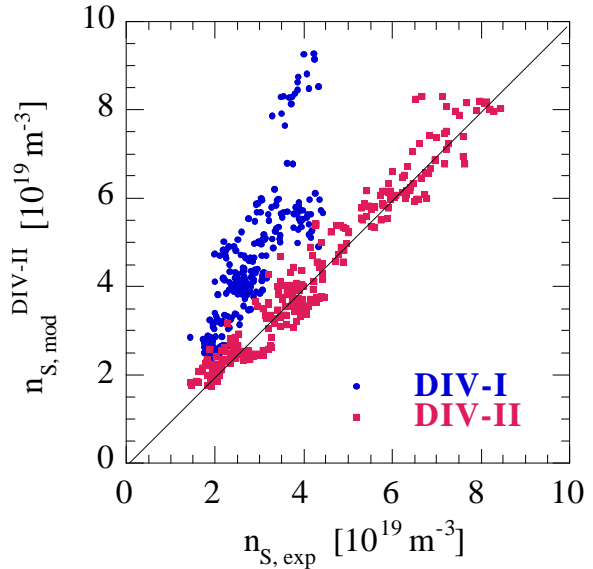


Fig. 3 Application of Equ. 7 with $x=II$ to both datasets in comparison to the experimental data points demonstrating the differences found for both divertor geometries.

In fig. 2 we compare results from the fit (equ. 6) and the model (equ. 7) respectively for the DIV-I database. A better ordering of the data points by the fit can be noticed. Comparing the exponents in equ. 6 and 8 the more pronounced q_{95} dependence of the fit is the major difference. This may at least be partly due to the small variation of B_t and q_{95} in the DIV-I dataset. For the DIV-II dataset the exponents of the model have been closely reproduced by the fitting procedure and both scalings were practically indistinguishable when compared in the same way as in fig. 2 [1]. The difference in the operational window for n_s by changing the divertor geometry is also illustrated in fig. 2.

4. Discussion

There are various possible reasons for the observed differences between DIV-I and DIV-II. One would expect a too strong q_{05} dependence if n_s is determined radially outside the true separatrix position. The effect of shifting the separatrix position is illustrated in fig. 4 where the scaling found for DIV-II (equ. 7, $x=II$) is compared to the experimental DIV-I densities taken 1 cm inside the nominal separatrix position. Doing this one single relation would describe both datasets and no differences would occur.

Such a big systematic error in the separatrix position between the DIV-I and DIV-II phase is, however, very unlikely as has been checked by analysing high resolution T_e profiles [3,5] and comparing them to various SOL models. From this study one would estimate an error of the separatrix position of only a few mm. Therefore, such errors are unlikely to be the main cause for the observed differences.

Another possible reason might be a systematically smaller pedestal width δ in DIV-I than in DIV-II. Because of equ. 2 this would give an effect in the right direction. The example profiles given in fig. 1 are at least consistent with this view, but much more analysis is needed to clarify this point.

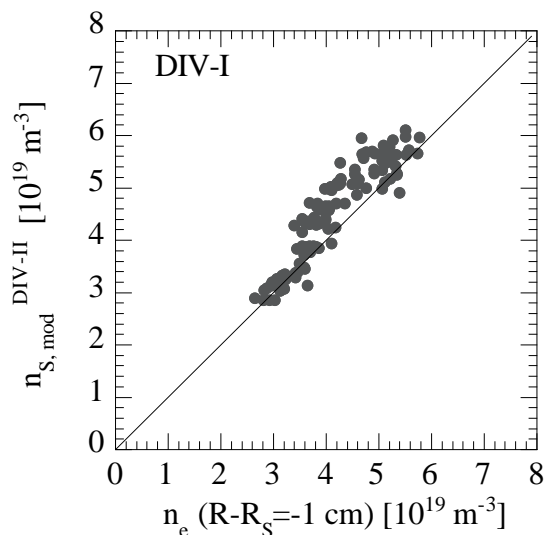


Fig. 4: $n_{s,mod}$ of equ. 7 with $x=II$ versus experimental density data points taken 1 cm inside the magnetically defined separatrix position of the DIV-I dataset (reduced number of points).

5. Summary and Conclusions

On the basis of AUG edge data for both divertor geometries, the scaling of the ratio n_s/n_c with respect to machine and discharge parameters was investigated with a view to the impact of the divertor configuration. The discussion was guided by a semi-empirical model which emphasises the impact of SOL physics. We have looked for scalings in terms of the parameters suggested by the model. With this approach fits for DIV-I and DIV-II data are of similar type and in good agreement with the model predictions.

The main difference between the scalings for DIV-I and DIV-II is the coefficient of proportionality which differs by a factor of 1.6. At present we are unable to discriminate between the different possible causes for this phenomenon.

References

- [1] K. Borrass, J. Schweitzer, J. Lingertat, *Scaling of the Separatrix to pedestal Density Ratio in ASDEX Upgrade H-Modes*, to be published. in Nucl. Fus.
- [2] H.-S. Bosch et al., Plas. Phys. & Contr. Fus. **41** (1999) A401-A408
- [3] J. Schweitzer et al. J. Nucl. Mat. **266-269** (1999) 934-939
- [4] J. Schweitzer et al., in Controlled Fusion and Plasma Physics (Proc. 22nd Eur. Conf. Bournemouth 1995), **19C**, III, European Physical Society, Geneva (1995) 253
- [5] J. Neuhauser et al., "Analysis of high-resolution ASDEX Upgrade edge plasma profiles", EPS99, this conference